Egyptian Geophysical Society
EGS Journal, Vol. 8, No. 1, 13-23 (2010)

GEOPHYSICAL AND STRUCTURAL STUDY ON GABAL ROD EL–BIRAM AREA, SOUTH EASTERN DESERT, EGYPT

A.H. Adly, M.A. Ragab, and A.E. Mohamed
Nuclear Materials Authority, P.O. Box 530 Maadi, Cairo, Egypt

دراسة تركيبية و جيوفيزيائية على منطقة جبل روض البيرام، جنوب الصحراء الشرقية، مصر

الخلاصة: تقع منطقة جبل روض البيرام فى جنوب الصحراء الشرقية بمصر بين خطى عرض ٠٠' ٢٥° ، ١٠' ٢٥° شمالاً وبين خطى طول ٥٠' ٣٣°، ١٠' ٣٤° شرقاً. تتميز منطقة الدراسة بالطبوغرافيا البسيطة والوعرة. تتراوح أعمار الصخور الظاهرة على السطح ما بين عصر ما قبل الكمبرى وعصر البليوزويك الأولى. حيث تتمثل صخور القاعدة الموجودة بالمنطقة بصخور السربنتين والصخور المرتبطة به وصخور الميتاجابرو والدايوريت المعقدة والصخورالبركانية المتحولة وكذلك الصخور الرسوبية المتحولة.

لدراسة التراكيب الجيولوجية التحت سطحية لمنطقة الدراسة وكذلك العلاقة بينها وبين التراكيب الظاهرة على السطح، تم تحديد العناصر التركيبية لكل من الخريطة المغناطيسية المحولة إلى القطب الشمالى المغناطيسى، والخرائط الناتجة من تطبيق تقنية التتبع التصاعدى المستمر. وهذا بالإضافة إلى تطبيق معامل الإلتفاف لأويلر.

إتضح من الدراسة أن صخور القاع الموجودة بالمنطقة هى السبب الرئيسى فى وجود معظم الشاذات المغناطيسية بالمنطقة.كما إتضح من تطبيق تقنية منحنى القوة الطيقية المحلية أن هناك مركبتين مغناطيسيتين رئيستين بالمنطقة، الأولى هى القريبة من السطح على عمق ٣٦٥ متر والأخرى عميقة على بعد ١,٢ كم من سطح الأرض.

تم رسم عدد من الخرائط الناتجة من تطبيق تقنية التتبع التصاعدى على مستويات مختلفة بدء من ٥٠٠ متر ثم ١٠٠٠ متر وأخيراً ١٥٠٠ متر. إتضح من تطبيق طريقة التحليل الإحصائى للاتجهات التركيبية على الخرائط المغناطيسية الموجودة، أن هناك خمسة إتجاهات تركيبية رئيسية تؤثر فى منطقة الدراسة وهى شمال – جنوب، شرق– غرب، شمال غرب – جنوب شرق، شرق شمال الشرق – غرب جنوب الغرب، شمال شمال الغرب – جنوب جنوب الشرق.

ABSTRACT: *Gabal (G.) Rod El-Biram area is located in the south Eastern Desert of Egypt, between lat. $25^o\ 00^/$ and $25^O\ 10^/$ N, and long. $33^O\ 50^/$ and $34^O\ 10^/$ E .The area under study is characterized by both gentle and rough topography. The exposed rocks belong mostly to the Late Precambarian age passing to Early Paleozoic age. The basement rocks in the study area are represented by serpentinites and related rocks, metagabbro - diorite complex, metavolcanics and metasediments.*

To evaluate the subsurface structural setting and the correlation between the surface and subsurface geological structures of the study area, the RTP map, upward continuation and Euler deconvelution techniques were applied.The structural elements deduced from the RTP map and upward continuation maps. The study illustrated that, the igneous basement rocks are the main causative bodies for the magnetic anomalies in the study area. Two main average interfaces, at depths of 0.365 km and 1.2 km, respectively, below the measuring level, were revealed through the application of local power spectrum on the RTP aeromagnetic map.

A series of upward continuation filters were applied on the RTP aeromagnetic data, using the coefficient computed by the numerical evaluation of the Fourier transform in the frequency domain. The computation were conducted on three different levels applying different grid cell units, which are compatible with 0.5 , 1.0 and 1.5 km average depths.

The statistical trend analysis illustrates five main structural trends of the mapped area. These trends have the directions NE, E-W, NW, ENE and NNW.

INTRODUCTION

Gabal (G.) Rod El-Biram area is located in the south Eastern Desert of Egypt, between lat. $25^o\ 00^/$ & $25^O\ 10^/$ N and long. $33^O\ 50^/$ & $34^O\ 10^/$ E (Fig.1). The area under study is characterized by both gentle and rough topography. It is traversed by several wadies which trend mostly in a NE-SW direction, as Wadi Beizah, Wadi Mueilha and G. Rod El-Biram which trend in the NW-SE direction. Many land marks exist in the area under study.

An airborne geophysical survey for the study area was carried out by Aero Service Division, Western Geophysical Company of Amerca in 1984.

It involved aeroradiometric survey, as well as aeromagnetic survey. Both surveys were conducted along parallel flight lines that were oriented in a NE-SW direction at 1.0 km spacing, while the tie lines were flown in a NW-SE direction at 10 Km intervals. To evaluate the subsurface structural setting and the correlation between the surface and subsurface geological structures of the study area, the RTP map, upward continuation and Euler deconvelution techniques were applied. The structural elements deduced from the RTP map and upward continuation maps. The igneous basement rocks are the main causative bodies for the magnetic anomalies.

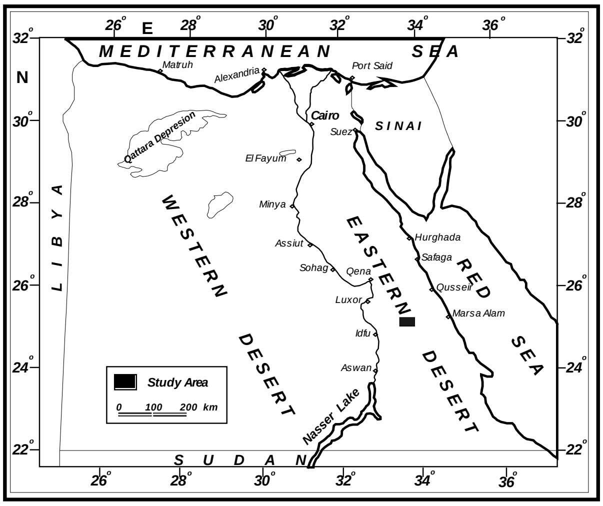

Fig. (1): Location map of Gabal (G.) Rod El-Biram area, south Eastern Desert, Egypt

AIM AND SCOPE OF THE STUDY

The study aims to the elucidation of the surface and subsurface geological and structural settings of the area. In order to attain this goal, the following steps were carried out:

1- Qualitative and quantitative interpretation of aeromagnetic survey data to help elucidate subsurface structures using various techniques of analysis which cover the topics of magnetic zones, upward continuation and Euler deconvolution.

2- Integration of all the interpreted results (aeromagnetic, structural and geological) which would lead for understanding the mode of occurrence and distribution of the subsurface structures.

GEOLOGIC SETTING

The distribution of the different rock types exposed in the area under study is given on the compiled geological map (Fig. 2). The area is surfaced almost by igneous and metamorphic rocks of the basement complex, traversed by several wadis filled with Quaternary and alluvial sediments. The exposed rocks are chronologically grouped into the following units, according to some modern classifications based on the works of (El-Shazly, 1964 and 1977, Stem, 1979, El-Shazly et al. 1980, Abdelmeguid, 1986 and El Gaby et al., 1988), started by the oldest:

1- Serpentinites and Related Rocks:

The serpentinites and related rocks are of wide distribution in G. Rod El - Biram area. They are found in the center and northern parts of the study area. These rocks are represented by serpentinite, talc-termolite – carbonates and talc magnesite rocks. The elongated serpentinite bodies trend predominantly in an ENE direction.

The serpentinites and related rocks are equivalent to the ultramafic magma associated with mafic volcanism (Hunting, 1967), as the member of ophiolite complex. The massive serpentines are a part of the pan African ophiolites (El- Gaby et al., 1988).

2- Metagabbro – Diorite Complex:

The metagabbro –diorite complex in the investigated area is of wide distribution and is found as elongated or irregular shape, nearly adjacent to serpentinites in most localities. The metagabbro –diorite complex was studied by EL-Ramly & Akaad (1960), and Akaad & Essawy (1964). It consists of dark green amphibole rich rocks, and characterized by marked variation in grain size and in the proportion of mafic to felsic minerals. The metagabbro –diorite complex consists primarily of uralitic amphibole, sometimes with relic cores of pyroxiene. The main rock types of the complex are relic gabbro, uralitized gabbro, metamorphosed gabbro, quartz diorites and amphibolites.

The metagabbro –diorite complex, sometimes directly overlies the serpentinites forming dislocated thrusted parts of an ophiolitic sequence. This rock unit appears certainly younger than the metasediments and metavolcanic rocks (Dardier, 1997).

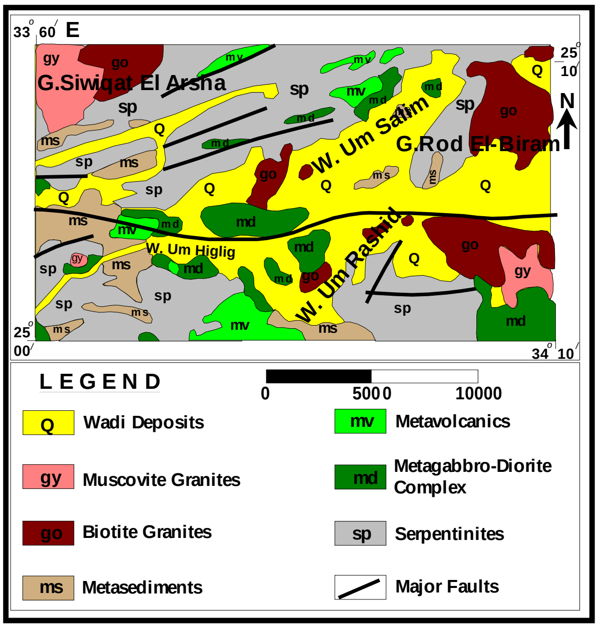

Fig. (2): Geological map of G. Rod El - Biram area, south Eastern Desert, Egypt, (Geological Survey of Egypt, 1989).

3- Metavolcanics:

The metavolcanics were developed during the early stages of evolution of the geosyncline and commonly referred to as metavolcanics. These rocks are limited in distribution in the study area and usually form dispersed conical peaks and disconnected ridges. They commonly found as flows, sills and thick sheet like bodies, normally interbedded with the first basement or geosynclinal sediments (El-Shazly, 1977).

The metavolcanics are massive, compact and fine-grained rocks, porphyritic, non porphyritic, sheared and schistose varieties are common near the contact with metasediments (Yousri, 1995 and Dardier, 1997).

4- Metasediments:

The metasediments unit was first defined by El Ramly and Akaad (1960), as including a thick succession of mostly fine grained "geosynclinal" sediments mainly in a low grade metamorphism and occasionally reaching a medium grade metamorphism.

The metasediments in the study area are of volcanogenic origin, mainly derived from the arc-type metavolcanics and may be formed in back arc basins especially, which include ironstone bands (Sims and James, 1984).

The series of metasediments consists of hornblends schist at the base followed by progressively lower grade rocks including mica schists, greywackes and mudstones (El Ramly and Akaad, 1960).

5- Medium-grained biotite and hornblende-biotite granite:

These rocks, previously known as the pink granites, form isometrical, lenticular and sheet-like bodies, sometimes of a considerable size. They are composed of quartz (35%), microcline perthite (35%), zoned plagioclase (25%) and biotite (3-8%), with some relics of hornblende. It seems possible that, due to tectonic action, the rock becomes more compact than the normal massive variety and thus forms large continuous masses instead of isolated separate hills intervened by wide valleys (Sabet et al., 1976).

6- Muscovite granites:

They are formed as a result of the metasomatic alteration of the Gattarian granites. These rocks form several small masses or stock-shaped bodies confined to the tectonically weakened zones (Sabet et al., 1976). They possess yellow, white or faint pink colour and are generally fine to medium grained. These rocks are characterized by the glittering flanks of muscovite. These rocks are more or less massive, but locally crushed and tectonized.

7- Wadi deposits and detritus sands:

The Quaternary - Wadi deposits, consisting of detritus, sand, pebbles, and rare boulders are distributed over the study area and constitute the surficial cover in the main wadis and tributaries. These deposits are referred to as Pleistocene and Recent deposits (Coastal plain deposits). Sand is commonly present in abundance in all the wadies, and it includes some wind blown sands accumulated in certain places and showing wind ripple mark

Structures:

The mapped area is dissected by a number of normal faults, which are either concomitant with wadis and drainage lines or cutting through the country rocks. These faults mainly trend in a NW-SW direction.

Youssef, 1968, believed that, the most prominent structural lines in Egypt can be grouped under the following categories: faults parallel to the Gulf of Suez-Red Sea direction (N35ºW), faults parallel to the Gulf of Aqaba direction (N15ºE), faults that deviate 10º west of the directions of both the Gulfs of Suez and Aqaba (N 45º W and N5º E).

Kamel, (1983) interpreted the photolineaments from aerial photographs of G. Mueilha and concluded that, the lineaments portray the main trends WNW-ESE and NE-SW. faults have three main trends NW-SW, WNW-ESE and E-W and there is less dominant NE-SW trend.

Dardier, (1997) studied the northern part of the area under consideration and arrange the faults in decreasing older of magnitude as follows: N-S. N40ºW, N50ºE and N70º W.

DATA PROCESSING

Calculation of Power Spectrum for Interface Determination:

Filtering techniques that, include high and low-pass filters, were applied in order to recognize the shallow and deep sources responsible for the regional and residual fields. Isolation of the regional and residual magnetic anomalies in the studied area was carried out by using the band- pass filter technique. The aeromagnetic data were interpreted by means of the local power spectra, suggested by Cianciara and Marcak (1976). The application of this technique revealed that, the contribution of the aeromagnetic data is coming from two sets of sources at two interfaces; 0.365 km and 1.20 km, for shallow and deep-seated levels, respectively.

Upward Continuation:

According to Kellog, (1953), the term "potential field continuation" is used to describe the evaluation process. Continuation may be "upward" away from the sources, or "downward" toward the sources. Upward continuation is mathematically stable smoothing operation. Downward continuation is mathematically unstable process, involving the amplification of short wavelengths where the signal-to-noise ratio is typically low.

The result of upward continuation is the filtering of the magnetic effects of the deep-seated bodies from those of the near-surface ones. (Tasy, 1975).

The Fourier transform F (u,v,0) of a potential field measured on a horizontal plane at z = 0, can be converted into the Fourier transform of the same field measured on the plane z = h by a simple multiplication (Bhattacharyya, 1967).

$$F(u,v,h) = F(u,v,0) \exp\left(h\left(u^2 + v^2\right)^{1/2}\right) \quad (1)$$

If h is negative, the operation is upward continuation, if h is positive, the operation is downward continuation.

Caress et al., 1989 stated that, "the downward and upward continuations are a natural extension of the statistical algorithm".

The upward-continued field is sharper, and consequently allows for better resolution of underground rock distribution.

The upward continuation is the process by which the magnetic field data are analytically projected from one datum surface upward to level surfaces above the original datum i.e., mathematically transformed into what it would be if it would be measured above the earth's surface (Blakely, 1995).

Upward continuation of potential fields represents a very interesting way to enhance the information content of a gravity or magnetic map. The increase of resolution, shared with many recent methods involving the use of directional derivatives. (Fedi et al,. 2002).

Filtering methods based on the Fourier transform are routinely used in the processing of geophysical data. Because of the nature of the Fourier transform is calculated. This preparation usually takes the form of removal of any trend from the data. The methods upward and downward continuations allow the control of both FFT-induced noises and other noises that are intrinsic to the dataset (Cooper, 2004).

Magnetic anomalies are sensitive to the variations in the size, depth and composition of the magnetized sources. A common approach to improve resolution of magnetic data is to compute the magnetic anomaly to a level close to the sources by means of upward continuation. Therefore, it is desirable to enhance the short wavelength and local long wavelength anomalies caused by sources at the different depths. This process improves at observation points on the horizontal planes below the measuring level (Bulent et al., 2008).

Euler Deconvolution:

3D Euler deconvolution is a technique applied to the gridded potential field data (Reid et al., 1990) to determine the position, depth and nature of any source present. The method is a generalization of EULDPH algorithm, that was applied to profile data in Thompson (1982). The method solves Euler's homogeneity equation for source position, working on a moving window of the grid:

$$(x-x^o)\, \partial_T / \partial_x + (y-y^o)\, \partial_T / \partial_y + (z-z^o)\, \partial_T / \partial_z = N(B-T) \quad (2)$$

where (x^o, y^o, z^o) is the position of a magnetic source, whose total field T is detected at location (x,y,z).

The total field has a regional field B;

N is the degree of homogeneity and may be interpreted as the structure index (SI) that is a measure of the rate of change of the potential field with distance and is related to the shape of the body.

The optimum source location is found by least square inversion of the data within a chosen window length. Solutions are generally obtained for different SI values (values between 0 to 3) and the solutions with best clustering of the data are selected. The advantages of this method, compared to other classical methods, for depth estimation are:

1. No particular geological model is assumed, and
2. Euler's equation is insensitive to magnetic inclination, declination and remenance (Rajaram, and Anand, 2003).

Higher values of the structural index (2 to 3) are more representive of two - and three – dimensional magnetic bodies, while lower values (0.5 to 1.5) are more representive of contacts and faults (Best et al., 1998).

Trend analysis:

One of the most useful geologic applications of magnetic survey is to definite the structural trends by following the lineation in magnetic contours (Dobrin , 1988).

The Rose diagram technique is a simple and standard method for portraying the two dimensional pattern and to construct a frequency plot showing the percentage of trends lying in various direction ranges (Miller and Khan, 1962). The trends of the lineations were grouped in 10-degree classes, and their lengths or numbers within a class were summed up and calculated as a percentage of the total lengths or numbers of all trends. The frequency distribution was constructed with respect to direction (clockwise and anticlockwise from the north).

The purpose of this analysis is to deduce the relationship between the geophysical lineament patterns and the tectonic setting in the study area, where the magnetic and tectonic patterns are well developed, statistical analysis of the three levels of the upward continuation and R.T.P maps. Lineaments indicating structural features were quantitatively carried out using the statistical rose diagram technique.

DATA INTERPRETATION

Qualitative Interpretation:

The careful examination of the RTP magnetic map (Fig. 3) shows that, the investigated area is characterized by the presence of groups of major and minor positive and negative magnetic anomalies of varying sizes and magnitudes. These groups of anomalies are mostly associated, on the surface, with intrusive bodies in these parts of the study area. The variation in amplitudes of these magnetic anomalies may reflect changes in the composition of these intrusions. Meanwhile, the differences in sizes of the anomalies reflect the extensions of the various intrusions.

The foregoing discussion exhibits the close agreement with the results obtained from the power spectrum.

It was possible to group the magnetic anomalies of the R.T.P. magnetic map (Fig. 3) into three magnetic anomalous zones. This zonation is based on the variation in the wavelength, amplitude, trend pattern and grouping of anomalies.

Here follows is a discussion of these three different magnetic zones:-

Magnetic zone No. 1:

The magnetic zone No.1 (Fig. 3) is generally consists of relatively lower-amplitude, negative magnetic character on the R.T.P. aeromagnetic map (Fig. 3) with two positive magnetic anomalies. This zone is located in the eastern, central and western parts of the area under study. These anomalies are characterized by moderate frequency and amplitude, which ranging between -400 and -500 nT. It is represented by circular shape.

Magnetic zone No. 2:

The magnetic zone No 2 (Fig. 3) was composed of positive magnetic anomalies. This zone shows clearly two systems of linear magnetic anomalies of pronounced, more or less moderate amplitudes and frequencies and constant direction (N30- 35W) , approximately parallel to the Red Sea as general axis. These two system of anomalies extend from SE to the mid northern of the study area.

The character of the magnetic anomalies may correspond to two buried systems of dykes of considerable dimensions, which had been intruded along two adjacent and parallel tectonic (shear zone).

The two mentioned systems are divided off and dislocated by another system of NE-trending system.

Magnetic zone No. 3:

It is characterized by high and very high positive magnetic anomalies (more than 1000 nT) in the southwestern, western and northern parts of the study area. They are associated with basic rocks, which characterized by high frequencies and amplitudes trending in different directions. The local variation of the frequency and amplitude of the magnetic anomalies are due to the difference in composition of geological units or the relative depth of their sources.

Quantitative Interpretation:

Two main average interfaces, at depths of 0.365 km and 1.2 km, respectively, below the measuring level, were revealed through the application of local power spectrum (Fig. 4) on the RTP aeromagnetic map (Fig. 3).

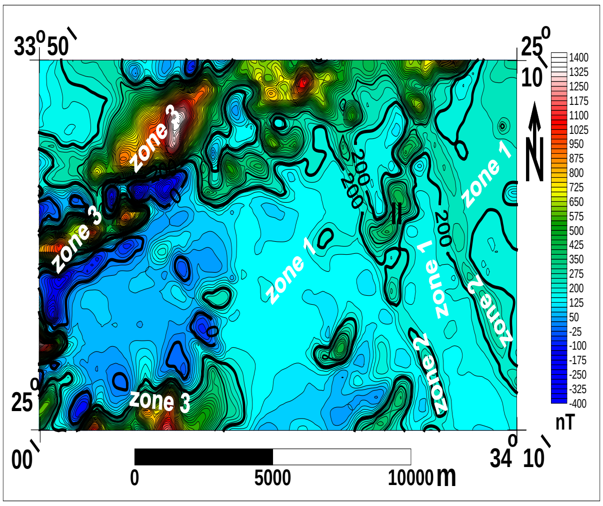

Fig. (3): Reduced to pole (RTP) magnetic intensity map, G. Rod El-Biram area, Southeastern Desert, Egypt.

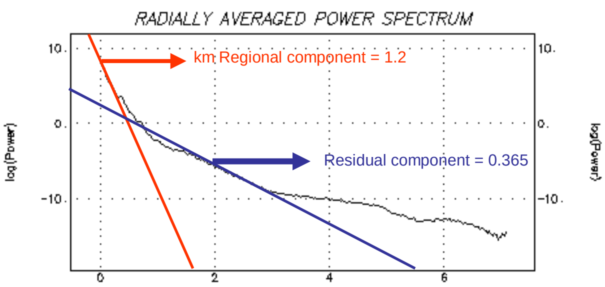

Fig. (4): Two – Dimensional local power spectrum of the RTP aeromagnetic map, G.Rod El-Biram area, south Eastern Desert, Egypt.

Upward continuation:

A series of upward continuation filters were applied on the RTP aeromagnetic data (Fig. 3), using the coefficient computed by the numerical evaluation of the Fourier transform in the frequency domain.

The computation were conducted on three different levels applying different grid cell units (grid spacings), which are compatible with 0.5 , 1.0 and 1.5 km average depths.

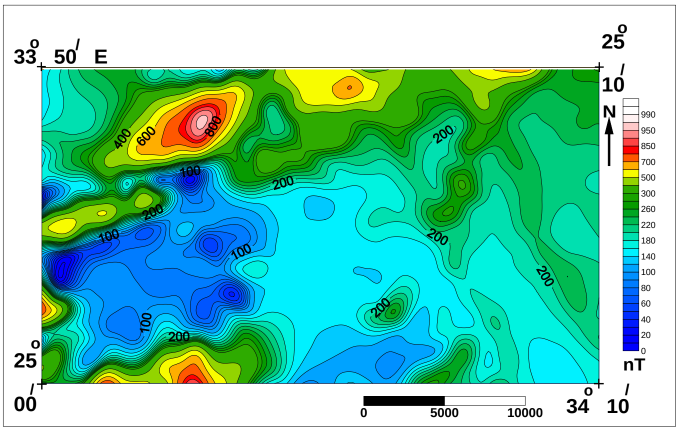

Fig. (5): Upward continuation map at level 0.5 km of G. Rod El-Biram area, south eastern Desert, Egypt

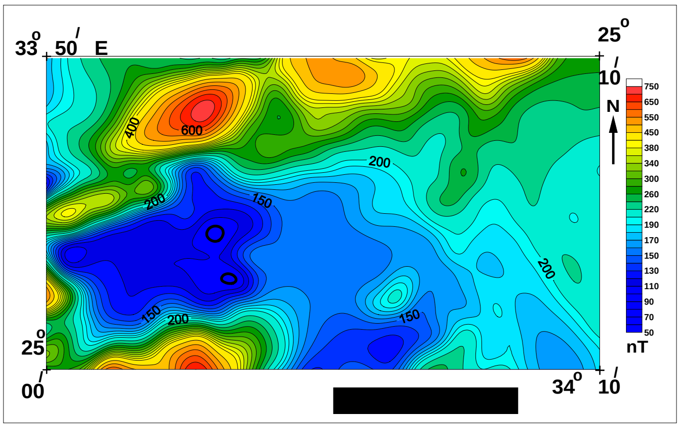

Fig. (6): Upward continuation map at level 1.0 km of G. Rod El-Biram area, south eastern Desert, Egypt

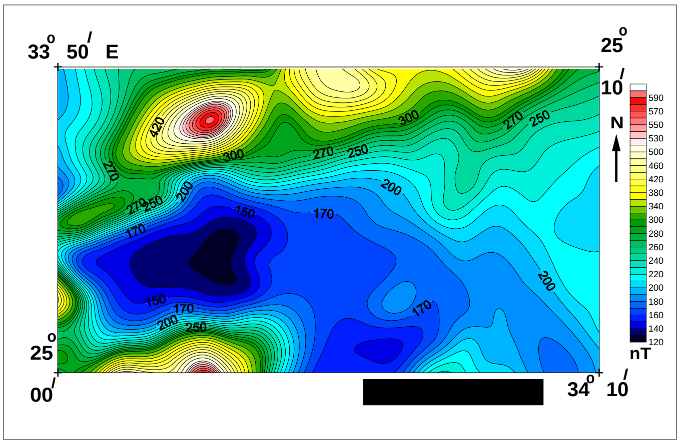

Fig. (7): Upward continuation map at level 1.5 km of G. Rod El-Biram area, south eastern Desert, Egypt.

The upward continuation maps (Figs.5 to 7) attenuate these shallow source anomalies and emphasize the deeper ones.

The upward continued map at level 500 m (Fig. 5) shows that, the western part in the study has high magnetic values and characterized by high magnetic relief and high amplitude. The high frequency and amplitude of this part may suggest its association with basic causative source, which is related on the surface with serpentinites, metagabbro-diorite complex, metavolcanics and metasediments. The western part is bordered from the central part by relative low magnetic anomalies. The positive magnetic anomalies in the western part are mainly striking in the NE-SW direction with some local deviation to the NNW, ENE and E-W directions of some anomalies. Meanwhile, the eastern part reflects relative low magnetic characters and shows the presence of two elongated features (may be basic dykes), which trending mainly in the NW-SE direction (Gulf of Suez-Red Sea trend) and affected by a set of NE-SW fault system. This feature is not present in the surface geology. Therefore, they are originated as deep-seated features (deep root).

The upward continued map at level 1.0 Km (Fig. 6) shows the existence of high and low magnetic zones, nearly at the same localities, that have been observed on the upward continued map level 0.5 km (Fig. 5).

Some of these magnetic anomalies are shown to be limited in extension at depth 1.0 Km and most of the residual bodies are removed. In the western part, the two high magnetic anomalous zones are separated by a low magnetic characters zone, which may reflect acidic intrusion or subsided zone. The two basic dykes in the eastern part became lower in magnetic characters and their sites reflect two major faults in the NW-SE direction.

The upward continued map at level 1.5 km (Fig. 7) shows broader effects of the proper deep-seated magnetic features including structural and lithologic variations within the basement allover the mapped area. The sources of high magnetic anomalies appearing on this map may indicate that, they are deeply-rooted.

The general view of these deep-seated magnetic characters, when passing from the first to the third levels, show that, their areal extent becomes wider and broader at the subsurface due to their long wavelengths and high frequencies. Close inspection of the three upward continued maps (Figs. 5 to 7) shows that, some of the low (or high) magnetic zones increase in their areal extent one the account of the high (or low) magnetic zones by increasing the depth of observation. The predominant structural trends deduced from the three upward continued magnetic maps (Figs.5 to 7) are the NE-SW, NW-SE, E-W and NNE-SSE directions. Therefore, they are expressed as deep-seated features in the study area.

The purpose of this analysis is to deduce the relationship between the geophysical lineament patterns and the tectonic setting in the study area, where the magnetic and tectonic patterns are well-developed. Lineaments indicating structural features were quantitatively carried out using the statistical rose diagram technique.

Euler deconvolution:

Applying the Euler deconvolution technique to the grided aeromagnetic data of the study area offers a good mean of interpreting contacts, faults and causative source bodies depending on the pre-selected structural index (S1), which identifies the rate of change of potential field with distance.

Two structural indices (S1) have been selected, as 0 and 1 characterizing contacts and dykes, respectively, and two maps have been constructed (Figs. 8 & 9) with coloured circles to depths at the source positions.

In the present study, the extended Euler deconvolution was run twice; one with a structural index (SI) of (0) to identify the magnetic contacts, and the other with (SI) equal (1.0) to identify sills and dykes. The Euler solutions, as seen in Figures (8 &9), would give an idea about the depth estimate of the magnetic sources. The deduced results for the magnetic contacts are shown on Fig. (8) and those for the sills and dykes on Fig.(9). The first map (Fig.8) shows different colors of circles and clustering exhibiting varying depths and trends of the main contacts of the plutons in the study area.. These contacts may reflect, in most plutons, faults taking many directions on different levels of depths , The shallower faults (60-160m) which reflect the contacts are shown over G. Abu Meriwa in the southwest of the study area and some parts of the gabbroic rocks in the southeast of the area. These faults take a NE-SW , E-W and NW-SE directions. The intermediate depths (contacts of 160-450m depths) are distributed allover the study area and take many directions as NE-SW , E-W , NW-SE, NNW-SSE and NNE-SSW. The deepest contacts (450-550 m) are recorded as structurally controlled and take a NNW-SSE , E-W and many other directions in minor amounts.

The second map (Fig.9) (SI = 1) is different from the first, with more deeper depths and linear clusters at different locations, suggesting the penetration of the interpreted faults to deep levels. The depth results obtained from the depth determination techniques reflect that the deepest faults (850 – 1000 m), are restricted in the eastern part of the map reflecting the intrusion of the basic dykes in this part and takes NNW-SSE and NW-SE directions, beside the E-W direction specially in the southwestern part of the mapped area over G. Abu Meriwa. Meanwhile, the intermediate and shallower depths of most dykes (200-850m) are distributed allover the study area and take many directions as NNW-SSE, NE-SW, E-W, ENE-WSW and N-S. These trends represent minor faults in some parts or major faults in other parts.

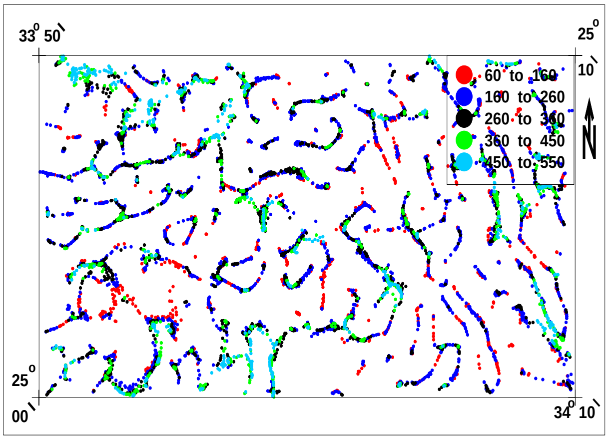

Fig. (8): First Euler 3D deconvolution map (SI=0), contact model of G. Rod El-Biram area, south eastern Desert, Egypt.

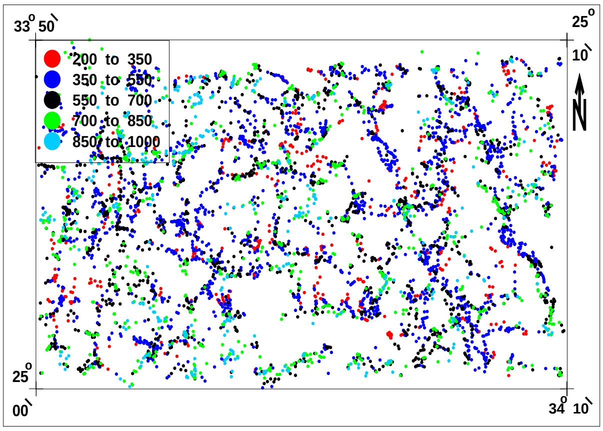

Fig. (9): First Euler 3D deconvolution map (SI=1), dyke mode of G. Rod El-Biram area, south eastern Desert, Egypt.

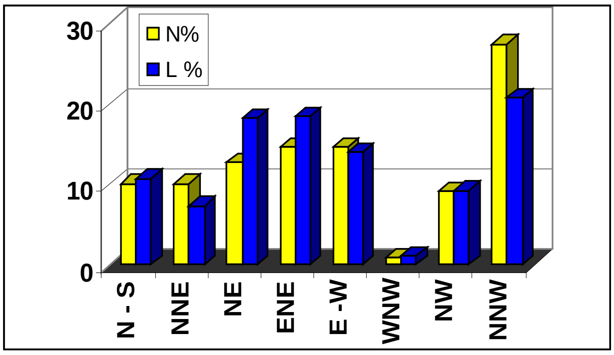

Fig. (10): Vertical bar chart showing lengths (L %) and numbers (N %) of relative frequency distributions of the interpreted structural lineaments from the RTP aeromagnetic map (Fig. 3), map of G. Rod El-Biram area, south eastern Desert, Egypt

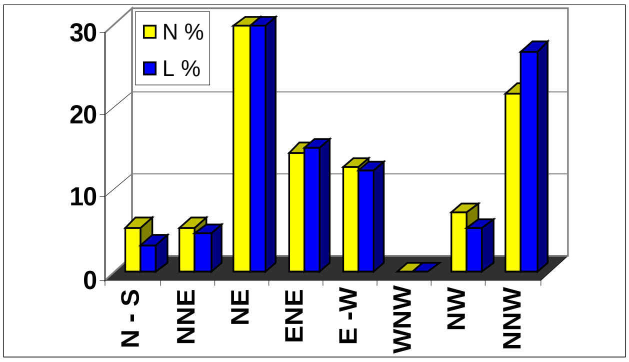

Fig. (11): Vertical bar chart showing lengths (L %) and numbers (N %) of relative frequency distributions of the interpreted structural lineaments from the Upward continuation map at level 0.5 km of G. Rod El-Biram area, south eastern Desert, Egypt

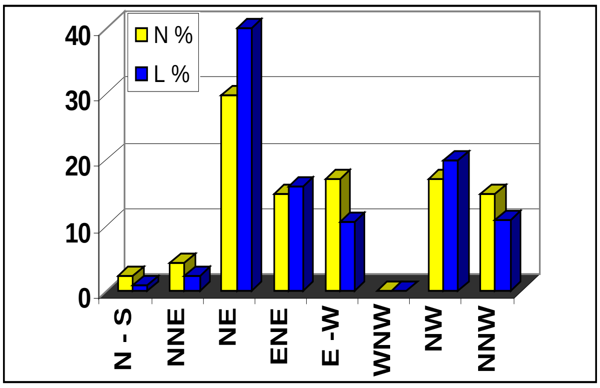

Fig. (12): Vertical bar chart showing lengths (L %) and numbers (N %) of relative frequency distributions of the interpreted structural lineaments from the Upward continuation map at level 1.0 km of G. Rod El-Biram area, south eastern Desert, Egypt

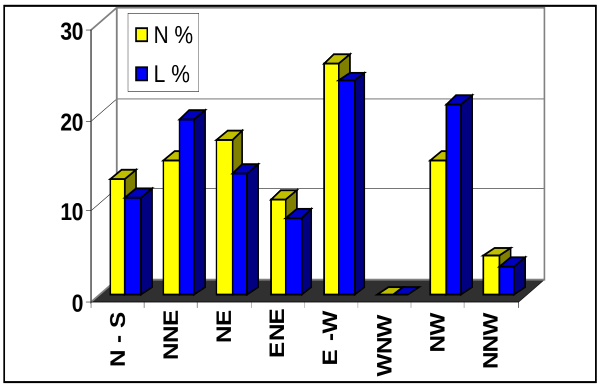

Fig. (13): Vertical bar chart showing lengths (L %) and numbers (N %) of relative frequency distributions of the interpreted structural lineaments from the Upward continuation map at level 1.5 km of G. Rod El-Biram area, south eastern Desert, Egypt

Trend analysis:

The four vertical charts (Figs. 10, 11, 12 and 13), could explain five main structural trends of the mapped area. These trends have the following common directions, NE, E-W, NW, ENE and NNW. These trends will be discussed in the following.

1- Syrian arc or Aualitic (NE-SW) trend:

This trend represents the Trans-African (Aualitic) trend and was developed as a major trend on the upward continued magnetic map at levels 0.5, 1.0 and 1.5 Km and as a moderate trend on the RTP magnetic map. The characteristic feature of this trend suggested that, it is originally formed during the Late Mesozoic time. The NE-block faults in the Central and South Eastern Desert of Egypt may be partly due to vertical and transcurrent movements.

2- Mediterranean or Tethyan (E-W) Trend:

This trend was recorded as a primary trend on the upward continued magnetic map at levels 1.0 and 1.5 Km and as a secondary trend on the RTP magnetic map and upward continued magnetic map at level 0.5 Km.

The prominent development of this trend on the magnetic map may refer to its existence at depth. The E-W trend is formed during Late Teriary time, where it started by the late Geosynclinal stage during the Precambrian Orogeny and an ancient fracture system resulting from a northern compression force.

3- Red Sea or Clysmic (NW-SE) Trend:

(NW-SE) Gulf of Suez – Red Sea (Clysmic or Erythrean) trend. This trend was developed as a moderate to weak trend on the RTP magnetic map, and as weak trend on the upward continued magnetic maps. This trend was interpreted as one of the fracture systems that, resulted from the force of a couple associated with the Red Sea and plays an important role in the structural history of Egypt and it formed during Early Teriary time.

4- Qattara (ENE-WSW) Trend:

This trend was developed as moderate trend on the RTP magnetic map and as a weak trend on the upward continued magnetic maps at levels 1.0 and 1.5 Km. This trend is an important basic dyke direction in parts of the exposed Arched basement of Egypt and it may have been rejuvenated during Hercynian Orogeny as a direction of compressional folding and upthrusting.

Meshref et al., (1973), noticed that, this trend shows a comparative strength on the Nubian side of the Red Sea rather than the Arabian side and considered to be the principal controlling direction of major folding in the unstable shelf running in a ENE direction from Libya to North Sinai. This direction is also a prominent direction of faulting and dyke intrusion in the exposed Precambrian terrain.

5- Atalla (NNW-SSE) Trend:

This trend was developed as a primary trend on the RTP magnetic map and as a secondary trend of the upward continued map at level 0.5 Km. According to the presence of this trend on the geological and magnetic maps, near surface as well as deep-seated structures. This trend may represent one of the shear fractures parallel to one of the sides of the faulted blocks, that resulted from the force of couple accompanying the formation of the great African right system associated with the Red Sea.

CONCLUSION

The delineation of gross structural framework of G. Rod El-Biram area in the south Eastern Desert of Egypt, was reached through the integration of some interpretation techniques applied to the aeromagnetic data. Two main average interfaces at depths 0.365 and 1.2 km below the measuring level were calculated by the computation of the local power spectrum of the magnetic data.

The upward continuation maps computed at three different levels (0.5, 1.0 and 1.5 Km) show the existence of high and low magnetic zones and most of the residual bodies are removed.

The application of Euler Deconvolution technique determined the depths of the causative magnetic bodies (contacts and sill & dykes), and trending in NNW, NE, NW, E-W and ENE directions.

Five sets of first order magnitude faults affected the mapped area, trending in NE (Trans-African), E-W (Mediterranean), NW (Gulf of Suez – Red Sea), ENE (Syrian arc) and NNW (Atalla) directions. These trends reflect a good agreement with the results obtained from the Rose diagram analysis techniques.

Finally the Euler Deconvolution and the upward continuation give additional constrain on the depth to the Precambrian basement and on the location of basement and intra sedimentary faults and magnetic bodies.

REFERENCES

Abdel Meguid, A.A. (1986): Geologic and radiometric studies of uraniferous granite in urn Ara Urn Shilman area. South Eastern Desert. Egypt. Ph.D. Thesis, Suez Canal Univ., 222 p.

Aero Services Division, Western Geophysical Company (1984): "Interpretation report of airborne gamma-ray spectrometer and magnetometer survey of the Eastern Desert of Egypt". pp.1-27.

Akaad, M.K. and M.A. Essawy (1964): The Meta - babbrodiorite complex NE of Gabal Atud, Eastern

Desert. Egypt. Bull.Sci. Techn., Assiut Univ. 7: pp. 83-108

Best, M., E., H.J. Abercrombie and J.W. pierce (1998): Interpreted faulting patterns in northeast Alberta using high resolution aeromagnetic data. Canadian Journal of Exploration Geophysicists. 10- 17 pp.

Bhattacharyya, B.K., (1967): some general properties of potential fields in space and frequency domain: a review: Geoexploration, 5, 127-143.

Boschetti, F., Hornby, P. and Horowitz, F., (2001): Wavelet based inversion of gravity data: Exploration Geophysics, 32, 48-55.

Blakely, R.J. (1995): Potential theory in gravity and magnetic application. Cambridge University Press, Cambridge, UK.

Bulent Oruc and Ayhan Keskinsezer (2008): Detection of causative bodies by normalized full gradient of aeromagnetic anomalies from east Marmara region, NW Turkey, Kocaeli University, Engineering Faculty, Department of Geophysical Engineering, 41380 Izmit-Kocaeli, Turkey.

Caress, David W.; Parker, Ropert L., (1989): Spectral interpretation and downward continuation of marine magnetic anomaly data, Journal of Geophysics Research, Volume 94, Issue B12, p. 17393-17404.

Cianciara P. and Marcak, H. (1976): Interpretation of gravity anomalies by means of local power spectra. Geophysical Prospecting, Vol. 24, pp. 273-280.

Cooper, G. (2004): The staple downward continuation of potential field data, Exploration Geophysics 35 (4) 260-265 p.

Dardier, A.M.A. (1997): Geology, petrography and radioactivity of some granitic masses in the area of Gabal Abu Diab, Eastern Desert, Egypt. Ph.D.Thesis, Faculty of Science, Ain Shamas University, 179 p.

Dobrin, M.B. (1988): Introduction to geophysical prospecting. Mc Graw-Hill Book Co., New York, 630p.

El Gaby, S., List, F-K., and Tehrani, R. (1988): Geology, evaluation and metallogensis of the Pan-African Belt in Egypt, in the Pan-African Belt of Northeast Africa and adjacent areas, ed. by S.El Gaby and R.O. Greiling, pp. 17-68. Friedr. Vieweg. Braunschweig . Federal Republic of Germany.

El Ram1y, M.F. and M.K. Akaad (1960): The basement complex in the Samut-Central Eastern Desert of Egypt between Lat 250º 30´ and 25º N. Geol. Surv. Egypt, Paper 8, 35p.

El-Shazly, E.M. (1964): On the classification of the Precambrian and other rocks of magmatic affiliation in Egypt. UAR. Section 10, International Congress, India, I 7 p

El-Shazly, E.M.(1977): The geology of the Egyptian region. In the Ocean Basins and Margins, Edited by Narin, A.E.M., Kanes, W.H., and Stehli, F.G., Plenum publishing corporation, pp.379-444.

El-Shazly, E.M., Dixon, T.H., Engel, A.EJ., Abdel Meguid, AA, and Stem, RJ.(1980): Late Precambrian crustal evolution of Afro-Arabia from oceanic arc to craton. Egypt. Jour. Geol., 24/1-2:pp. 101-121.

Fedi, M., and Florio, G. (2000): A stable downward continuation by using the ISVD method, Corresponding to presented at the 25th General Assembly of the European Geophysical Society, Nice, France, 25-29 April, 2000

Geological Survey of Egypt (1989): Geological map of basement rocks of Gabal Urn Gheig, Egypt, Scale 1:1 000000, Geol. Surv. Egypt, Cairo, Egypt, 1989, I map.

Herve Trompat, Fabio Boschetti and peter Hornby, (2003): Improved downward continuation of potential field data, Exploration Geophysics (2003) Vol 34, No. 4

Hunting Geology and Geophysics Ltd. (1967): Assessment of the mineral potential of the Aswan region, U.A.R. Photogeological surveys. U.N. Dev. progr; U.A.R. Regional Planning of Aswan. 138 p.

Jeffrey D. Phillips, (1994): Potential-field continuation: past practice vs. modern methods

Kamel, A.F (1983): Relation between photolineaments and radioactivity in Gebel El Mueilha Eastern Desert, Egypt: Journal of African Science.

Kellog,O.D. (1953): Foundations of potential Theory: Dover Publications, Inc.

Mallat, S. and Zhong, S. (1992): Characterization of signals from multiscale edges: IEEE Transactions on Pattern Recognition of Machine Intelligence, 14, 710-32.

Meshref, W.M. and Sheikh, M.M.(1973): Magnetic tectonic trend analysis in Northern Egypt. J. Geol., vol. 17, No.2, pp.184-197.

Miller, R.I. and Khan, I.S. (1962): Statistical analysis in the Geol. Sciences. Hohn Willey and Sons Inc., New York. USA, 429p.

Rajaram, M. and Anand S.P. (2003): C rustal structure of Southern India from aeromagnetic data. Journal of the Virtual Explorer, Vol. 12, pp. 72 – 82.

Reid, A.B., Allsop, J.M., Granser, A.J., Miliett, A.J. and Somerton W.I. (1990): Magnetic interpretations in three dimensions using Euler deconvolution. Geophysics, Vol. 55, pp. 80 – 91.

Sabet, A.H., V.V. Bessonenko and B.A. Bykov (1976): The intrusive complexes of the Central Eastern Desert of Egypt. Ann. GeoI.Surv.Egypt.6: pp. 53-73.

Sims, P.K. and James, H.L., (1984): Banded iron-fonnation of Late Proterozoic age in the Central Eastern Desert, Egypt: Geology and tectonic setting, Econ. Geol., 79, 8, pp. 1777-1784.

Stem, R.J. (1979): Late Precambrian ensimatic volcanism in the Central Eastern Desert, Egypt, Ph.D. Thesis, Univ. Cal. San Diega, 210p.

Tasy, L.J. (1975): The use of Fourier series method in upward continuation with new improvements. Geophysical Prosp., Vol. 23, pp. 28-41.

Thompson, D.T. (1982): EULDPH – A new technique for making computer assisted depth estimates from magnetic data. Geophysics,Vol. 47, pp. 31 – 37.

Yousri, M.M. (1995): Geology of the area around Gabal EI-Mueilha, Central Eastern Desert, Egypt. Ms. Sc Thesis (Geology Department, Zagazig University, 151 P.

Youssef, M.I. (1968): Structural pattern of Egypt and its interpretation. Am. Assoc. Petrol. Geol. Bull., V.52, pp. 601 -614